Study on PET/PP Microfibrillar Composites. I. Morphological Development in Melt Extrusion

X. D. Lin, W. L. Cheung

Department of Mechanical Engineering, The University of Hong Kong, Hong Kong, People's Republic of China

Received 8 January 2001; accepted 9 September 2002

ABSTRACT: Poly(ethylene terephthalate)/polypropylene (PET/PP) blends of different compositions were extruded through a 2-mm capillary die using a corotating twin-screw extruder. The extrudates were cryogenically fractured and examined using scanning electron microscopy. The viscosity ratio of the constituent polymers alone was found not suitable for explaining the polymer blend morphology. At a PET concentration of 20%, the extrudate consists of three regions: The skin layer, about 10 μm thick, has a lower concentration of the dispersed PET phase than that of the overall concentration. The intermediate region, about 400 μm thick, has profuse PET fibers and some small PET particles. The central region, approximately 800 μm in diameter, contains mainly PET particles that are generally bigger. A low barrel temperature, low die temperature, and fast cooling rate helped to retain the fibers near the extrudate skin. Meanwhile, variation of the barrel temperature, die temperature, and cooling media did not affect the PET particle-size distribution significantly in the central region of the extrudate. A high screw speed and a high postextrusion drawing speed were very effective in producing fibers in the extrudates through elongation of the particles. At a PET concentration of 30%, coalescence of the PET phase was prevalent, leading to the formation of PET platelets near the extrudate skin and irregular PET networks in the central region of the extrudate. J Appl Polym Sci 88: 3100–3109, 2003

Key words: morphology; blends; extrusion

INTRODUCTION

Morphology plays an important role in the mechanical properties of a polymer blend. A high degree of molecular orientation of the reinforcing polymer is essential in high-performance polymer alloys. In an extrusion process, the development of the blend morphology does not depend only on the intrinsic properties of the constituent polymers but also on extrinsic factors such as the melt-flow rheology through the die, the speed of postextrusion drawing, and the rate of cooling of the extrudate. In the development of the so-called molecular composites, liquid crystalline polymers (LCPs) have been studied extensively because of their intrinsic ability to form fibrils in melt processing.[1–9] However, LCPs are too expansive for general engineering applications. On the other hand, there are considerable supplies of poly(ethylene terephthalate) (PET) and polypropylene (PP) in the form of postconsumer scraps. These waste streams of PET and PP could be a low-cost source of raw materials for forming polymer blends.

Unlike LCPs, the molecules of common thermoplastics relax rapidly during melt processing; therefore, a high degree of molecular orientation is difficult to achieve. By adding 18–22% of PET to PP, Spreeuwers and van der Pol[10] produced a blend (AP-28) of fine PET fibers in a PP matrix with an extraordinarily high tensile strength. Probably due to processing requirements, AP-28 is only produced either in fiber or in ribbon form. There is little information about its ability to undergo conventional molding processes into other forms of products. More recently, some work was reported on PET/PA6 microfibrillar composites.[11–13] The polymer fibrils are created by drawing the polymer blend, leading to the orientation or fibrillization of both components followed by melting or isotropization of the lower melting component with preservation of the oriented microfibrillar structure of the higher melting component.

Presently, we are engaged in a study on the development of a PET/PP microfibrillar composite that can be processed by conventional molding methods. The ultimate objective is to develop a technology for recycling PET and PP. In this study, virgin polymers were blended in a twin-screw extruder to produce an extrudate with fibrous PET domains in a PP matrix. Subsequently, the extrudate would be drawn in a solid state, either at room temperature or at an elevated temperature, to further enhance the molecular orientation of the PET fibers to give a microfibrillar composite. Eventually, the processability of the composite by conventional molding methods at a temperature above the melting point of PP but below that of PET

Correspondence to: W. L. Cheung.
Contract grant sponsor: The University of Hong Kong.

Journal of Applied Polymer Science, Vol. 88, 3100–3109 (2003)

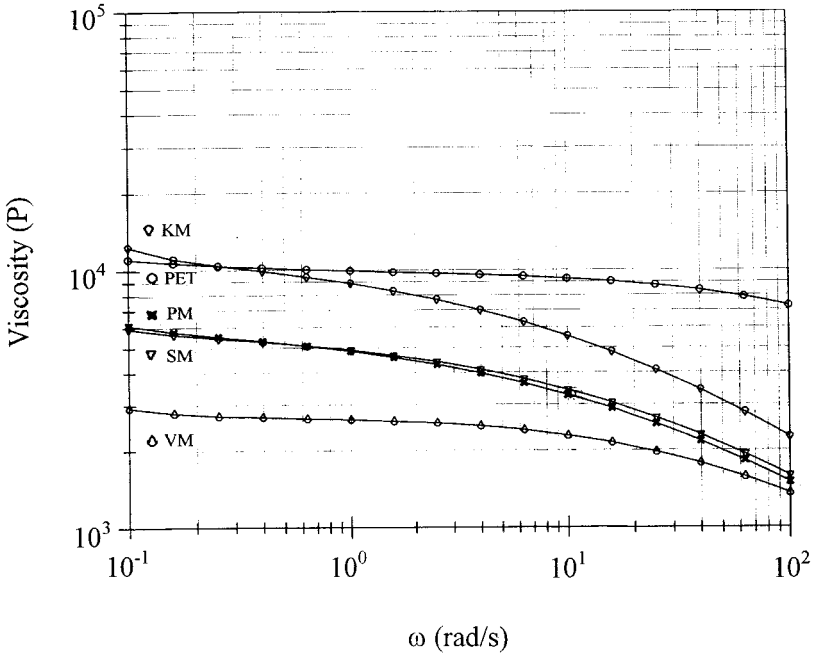

Figure 1 Effect of angular velocity of the stress rheometer on dynamic viscosity of PET and PP (KM, PM, SM, and VM) resins; testing temperature 270°C.

would be assessed. This article outlines the results on morphological development of the PET/PP blends in melt extrusion.

EXPERIMENTAL

Materials and processing

The isotactic PP resins used were KM6100, PM6100, SM6100, and VM6100 (Shell Chemicals, The Netherlands) in granule form. Their melt-flow indexes as provided by the manufacturer are 3.0, 5.5, 11, and 22, respectively. The PET resin was Arnite D04 300 by Akzo (The Netherlands), a medium-viscosity extrusion grade. The blending process was carried out in a Prism corotating twin-screw extruder (UK). It has a screw diameter of 16 mm and a length-to-diameter (L/D) ratio of 25. The capillary die has a diameter of 2 mm and a length of 10 mm (D2L10). Before blending, the PET resin was dried in an oven at 120°C for 4 h. It was then manually mixed with a predetermined amount of PP and fed into the extruder. There are four temperature-control zones (T_1, T_2, T_3, and T_4) along the barrel, with T_1 next to the hopper and T_4 next to the die. After some preliminary trials, a basic set of extrusion parameters were determined as follows: T_1 = 160°C, T_2 = 220°C, $T_3 = T_4$ = 270°C, die temperature = 270°C, screw rotational speed = 50 rpm, and postextrusion drawing speed = 15 m/min. The extrudate was cooled in a water bath at room temperature. To study the effect of a given extrusion parameter on the morphology of the extrudate, the concerned parameter was changed while other parameters were kept at the basic setting.

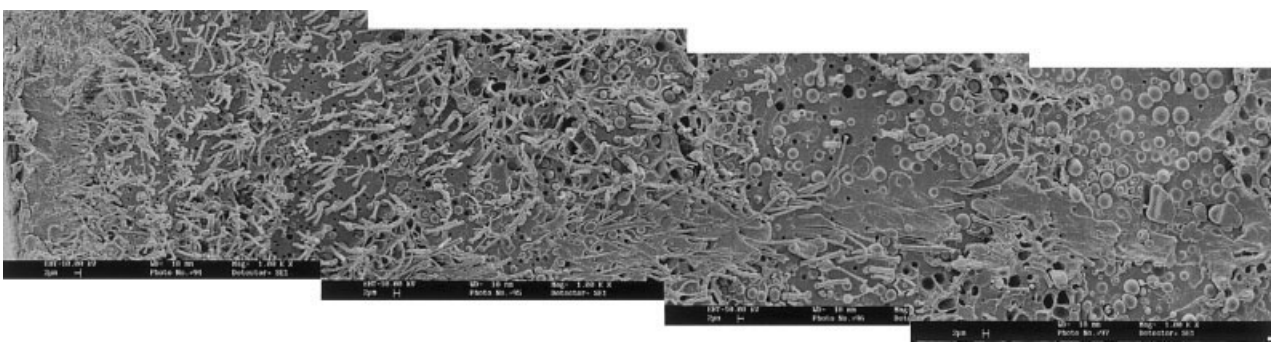

Figure 2 Cryogenically fractured cross section of a PET/VM (20/80) extrudate showing (left) PET fibers near the skin and (right) PET particles in the central region.

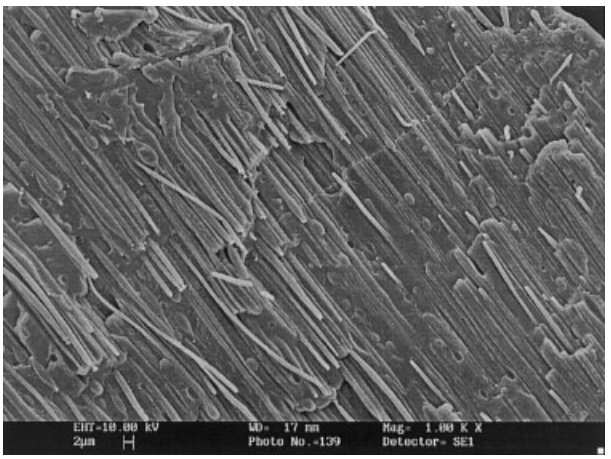

Figure 3 Longitudinal section near the skin of a PET/VM (20/80) extrudate prepared under the basic extrusion setting.

Viscosity measurement

The dynamic viscosities of the polymers were measured by a Rheometrics dynamic stress rheometer (SR-200) as a function of frequency at 270°C in nitrogen. The experiments were performed at a strain of 5% and the gap between the parallel plates was 1 mm.

Scanning electron microscopy

The morphology of the PET/PP extrudates was studied by a Cambridge S440 scanning electron microscope. The composite extrudates were cryogenically fractured by simple bending to give a cross-sectional view or by splitting to give a longitudinal view. The fracture surfaces were sputtered with a layer of gold–palladium before examination.

Measurement of PET fiber diameter and particle size

The diameters of the PET fibers within the extrudates were measured from SEM micrographs. More than

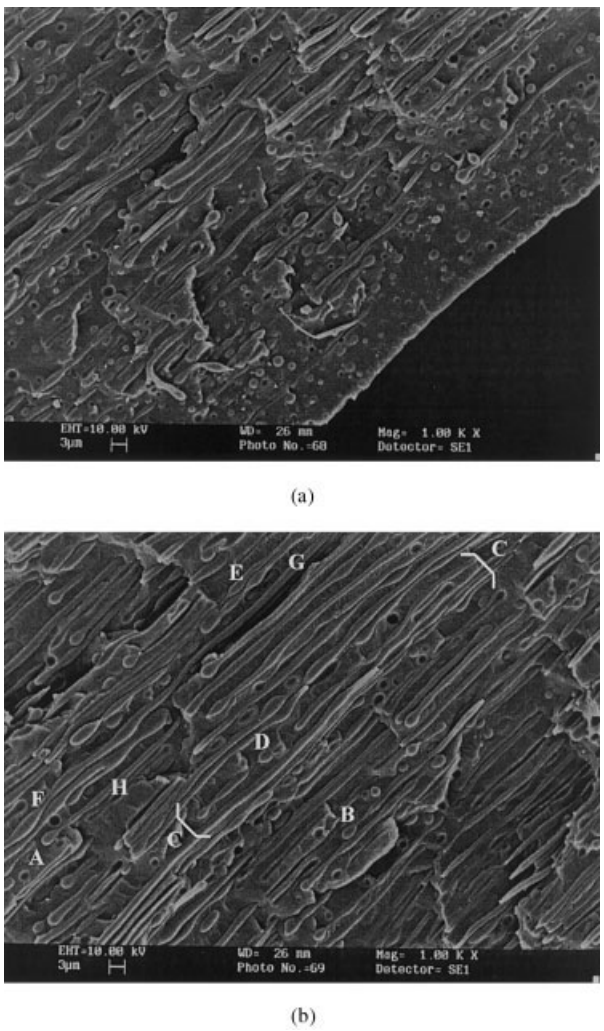

Figure 4 (a) Longitudinal section of the skin region of a PET/VM (20/80) extrudate; postextrusion drawing speed: 6 m/min. (b) Longitudinal section near the skin of a PET/VM (20/80) extrudate: (A,B) fiber ends breaking away from main body of the fibers; (bracket C) fiber breaking into several sections simultaneously; (D) broken fiber section shrinking into a particle; (E,F) neighboring fibers with conformable shapes; (G,H) coalescence of fibers; postextrusion drawing speed: 6 m/min.

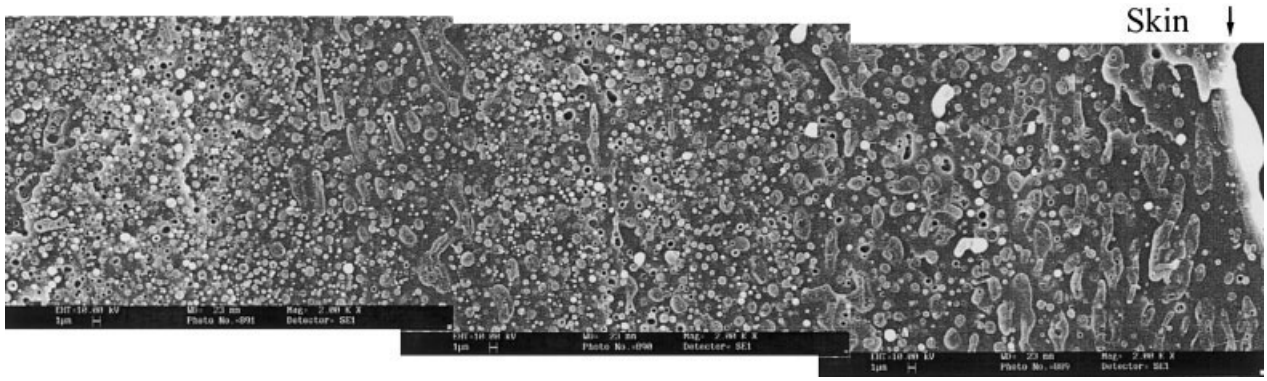

Figure 5 Cross section of a PET/KM (30/70) extrudate (right) skin and (left) halfway between the skin and the extrudate center.

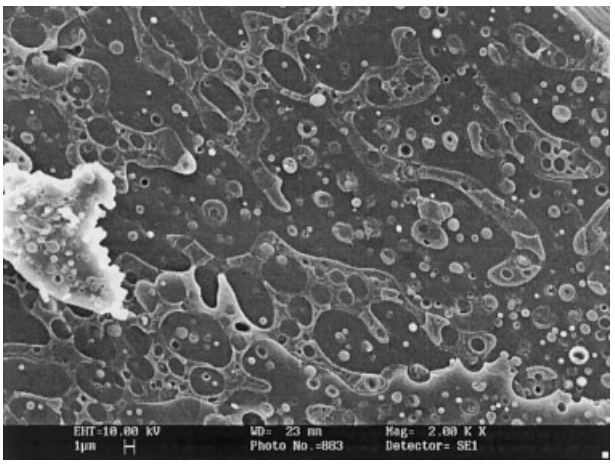

Figure 6 Central region of a PET/KM (30/70) extrudate showing PET networks with entrapped PP fibers.

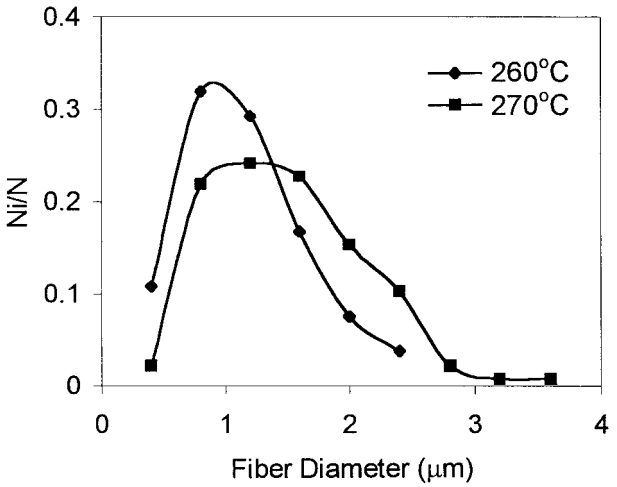

Figure 8 Effect of barrel temperature on PET fiber diameter distribution in PET/VM (20/80) extrudates.

200 measurements were taken for a given sample. The fibers were graded and then the ratio between the number of a certain grade (N_i) and the total number (N) of measurements was plotted against the fiber diameter to give a diameter distribution graph. Similarly, diameter distribution graphs were also obtained for PET particles within the extrudates.

RESULTS AND DISCUSSION

Effect of viscosity ratio

It was reported that the dispersed phase is more likely to form fibers during extrusion when the viscosity ratio (viscosity of the dispersed phase/viscosity of the matrix polymer) is close to unity.[14,15] Figure 1 shows curves of the dynamic viscosity versus frequency of the polymers. The viscosity ratio of PET/KM is closer to unity than are those of the other blend pairs within the tested range of angular velocities, ω, or "shear rates." At $\omega = 10^2$ rad/s, the viscosity ratio of PET/KM is approximately 3.7 and that of PET/VM is 6.8. According to Taylor,[16] a drop of fluid with a viscosity that exceeds the viscosity of the suspending fluid by a factor of more than approximately 4 does not become stretched in a simple shear flow, but, rather, achieves a steady, slightly deformed shape for all large shear rates. This suggests that PET/KM should give a more fibrous morphology than that of

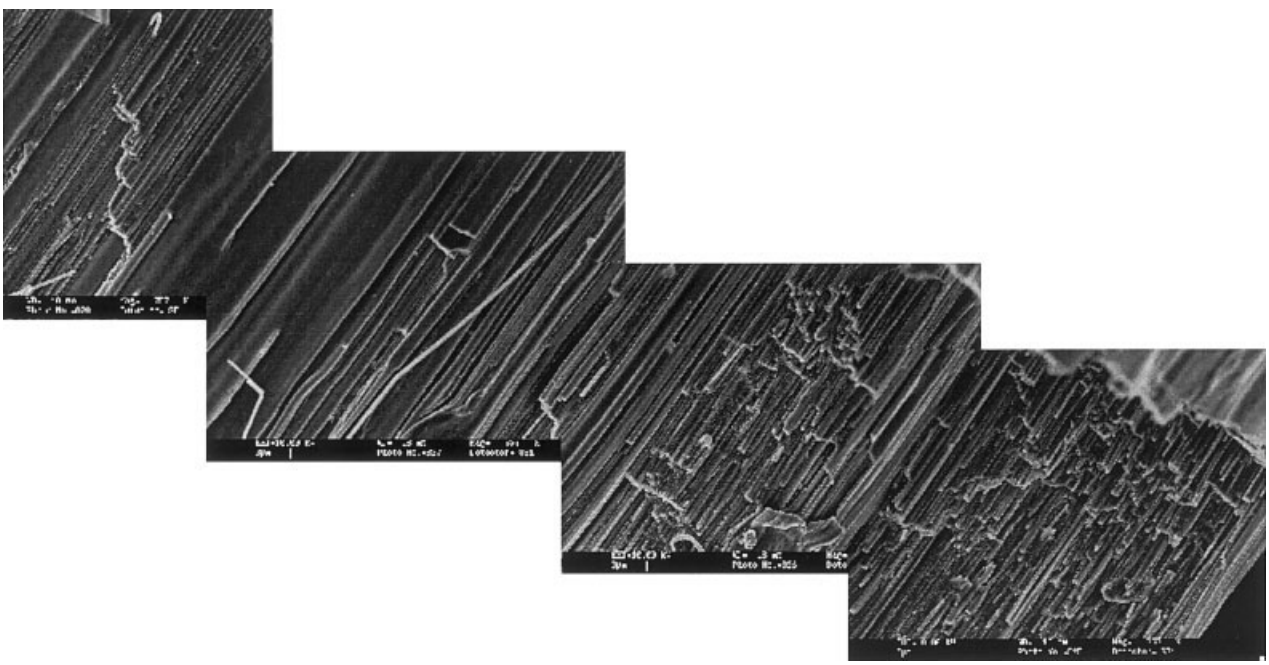

Figure 7 Longitudinal section of a PET/KM (30/70) extrudate.

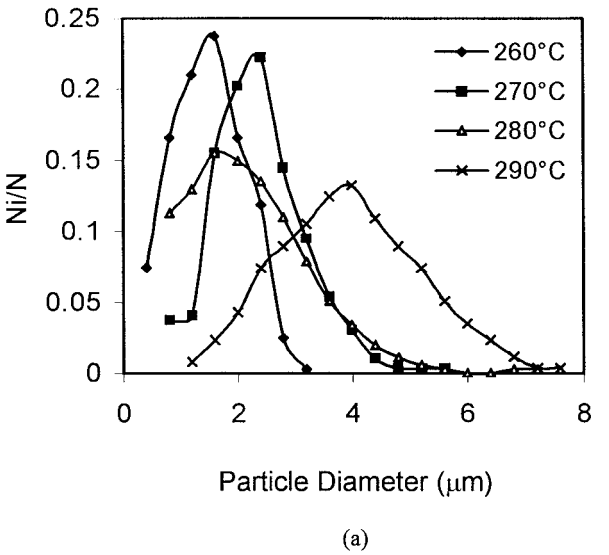

(a)

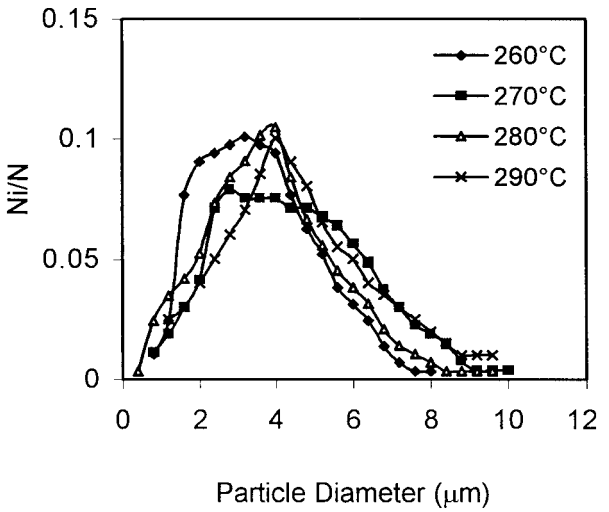

(b)

Figure 9 Effect of barrel temperature on PET particle-size distribution in PET/VM (20/80) extrudates: (a) near skin; (b) central region.

the other blend pairs and PET/VM should be less fibrous. On the contrary, more fibers were observed in the PET/VM blend than in any other blends under the basic extrusion setting. Perhaps the viscosity ratio alone is not suitable for explaining polymer blend morphology.[17]

Morphology of PET/VM(20/80) blend

Figure 2 shows a typical view along the radius of the cross section of the PET/VM (20/80) extrudate prepared under the basic extrusion setting. The region near the skin (left) contains many pulled-out PET fibers and some small PET particles. However, the number of fibers decreases toward the central region (right) of the extrudate, giving way to some large particles. Figure 3 shows the longitudinal section near the skin of the extrudate. The PET fibers generally have a diameter of about 1 μm and their length-to-diameter ratio is large. There are signs of necking at some of the fiber ends, which are caused during fracture of the extrudate.

Figure 4(a) shows the longitudinal section of another extrudate prepared under very similar conditions except at a lower postextrusion drawing speed of 6 m/min. There is a skin layer, ~10 μm thick, with a lower concentration of PET. This is probably a result of the migration of the dispersed PET phase toward the low stress in the capillary center.[18–20] Figure 4(b) shows another region near the skin. The phenomenon of capillary instability is obvious.[21] The enlarged fiber ends often break away from the main body of the fiber, A and B. A fiber may break into several sections

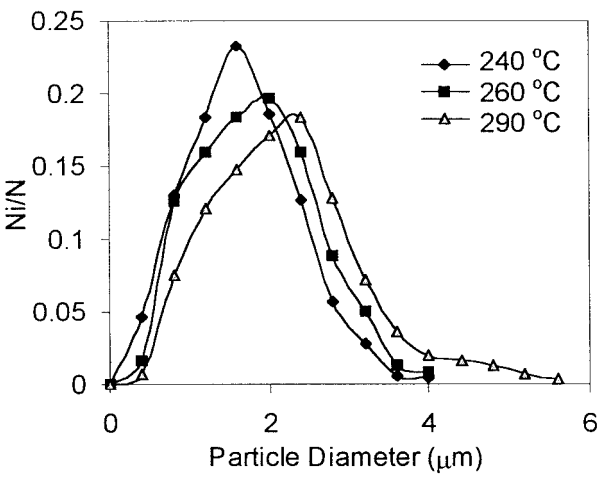

(a)

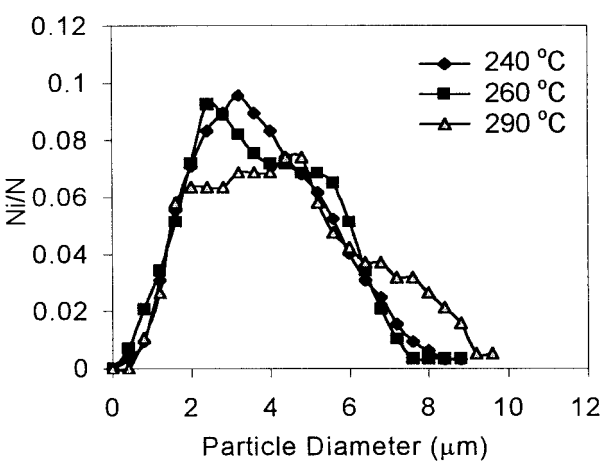

(b)

Figure 10 Effect of die temperature on PET particle-size distribution in PET/VM (20/80) extrudates: (a) near skin; (b) central region.

almost simultaneously, bracket C. The broken sections will then shrink into particles under the influence of interfacial tension, D. When two fibers are brought very closely together, their shapes become conformable with each other, E and F, and eventually the neighboring fibers may merge together, G and H.

Morphology of PET/KM (30/70) blend

Melt fracture occurred when extruding a blend of 30% PET and 70% KM6100, PET/KM (30/70), using the basic extrusion setting. When a die of diameter of 2 mm and length of 20 mm was used, the extrudate became smooth. The longer die (D2L20) allowed more time for the deformed PET phase to relax, hence reducing the degree of die swell and eliminating the phenomenon of melt fracture. Chapleau and Favis[22] found that too high an *L/D* ratio could not give a fibrous morphology in PC/PP (5/95) blends because of the recoil-back or recovery of the deformed phase.

Figure 5 shows the cross section of a PET/KM (30/70) extrudate from the skin to about halfway toward the center. A layered structure is observed. The layer next to the skin, approximately 70 μm thick, contains large domains of PET with an elongated cross section. These are, in fact, PET platelets with the long axis along the flow direction. They were formed as a result of coalescence. It was reported that when the minor-phase concentration was increased to 20% coalescence became obvious.[22] The PET platelets are approximately parallel to the circumferential direction of the extrudate, suggesting that coalescence tends to occur within layers of constant shear.

Further away from the skin, the elongated cross section of the PET domains gradually gives way to a circular cross section. This implies that most PET domains are now in the form of dispersed fibers or particles. This second layer has a thickness of approximately 60 μm. There are some holes within this layer, which is an indication of fiber pull-out. The third layer has a similar morphology as the first layer but the thickness is much smaller. It is followed by another fibrous region similar to the second layer. At present, it is not fully understood how such an alternating layered structure has developed; nevertheless, it should be related to the flow rheology through the die. Figure 6 shows the central region of the extrudate. Many of the PET domains are irregular in shape and some of them are merged together to form a network. Within these networks, some entrapped PP domains are found in the form of fine fibers.

Figure 7 shows a longitudinal view of the PET/KM (30/70) extrudate through the center. No obvious PET particles are seen, which strongly indicates that coalescence of the minor phase is prevalent at a concentration of 30%. The skin region (right) exhibits an extremely fibrous morphology, which is due partially to dispersed PET fibers and partially to the edge-on view of the PET platelets near the extrudate surface. The central region (left) gives a smooth filmlike structure. This can be explained by the fact that the PET platelets or networks in the central region are less oriented. During splitting of the extrudate, failure occurred along the PET/KM interfaces that were roughly parallel with the fracture plane. The clean fracture surface indicates that the adhesion between the polymers is poor.

Effect of barrel temperature

The effect of barrel temperature was studied by changing T_3 and T_4 while keeping other extrusion parame-

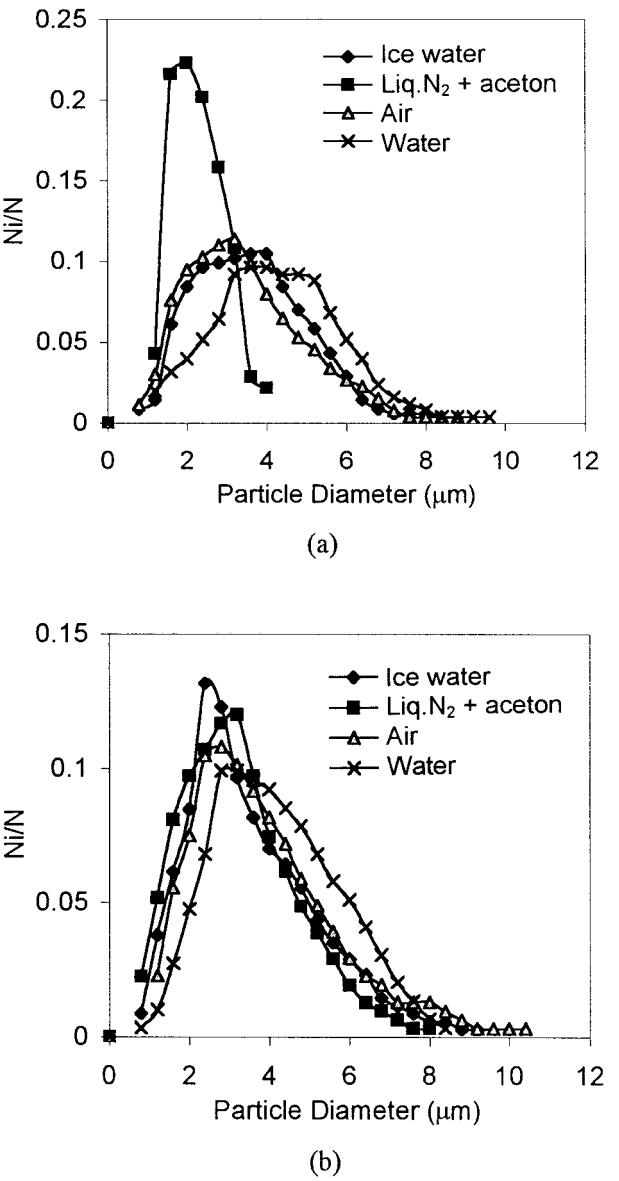

Figure 11 Effect of cooling media on PET particle-size distribution in PET/VM (20/80) extrudates: (a) near skin; (b) central region.

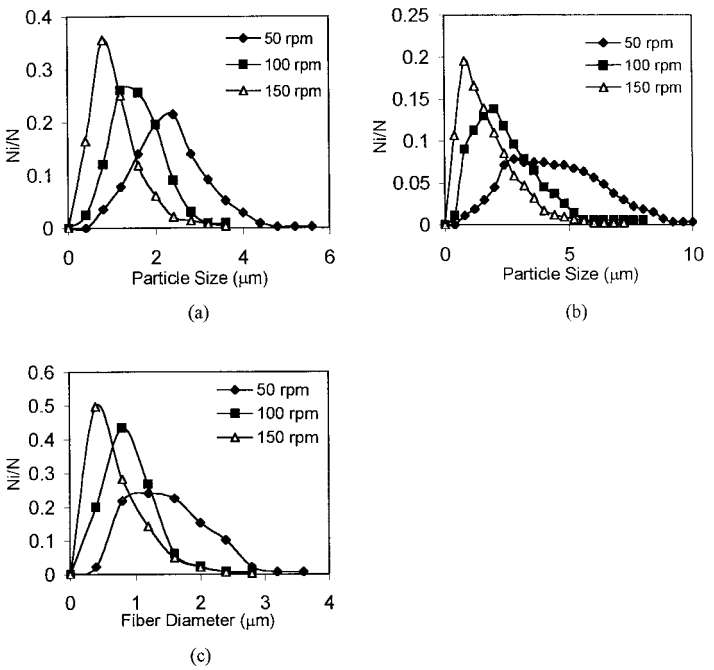

Figure 12 Effect of screw speed on domain-size distribution of PET phase in PET/VM (20/80) extrudates: (a) particle size near skin; (b) particle size in central region; (c) fiber diameter near skin.

ters fixed. Four temperature settings, namely, $T_3 = T_4 = 260$, 270, 280, and 290°C, were used. In general, the morphology for $T_3 = T_4 = 260$ and 270°C are similar (Fig. 2) and the fiber diameter distributions of the extrudates are shown in Figure 8. Apparently, a lower barrel temperature or melt temperature favors the formation of finer PET fibers. In contrast, there are basically no PET fibers but only particles in the extrudates prepared at 280 and 290°C. Vainio et al.[23] analyzed the particle-size distribution in order to optimize screw configuration for extrusion. In this study, the particle-size distributions both near the skin and in the central region were investigated for extrudates prepared at the different barrel temperatures. Near the skin [Fig. 9(a)], the particle size generally increases with an increasing barrel temperature; the peak particle size shifts from 1.5 μm for 260°C to 4 μm for 290°C. Also, a broader particle-size distribution is observed for the higher barrel temperature. In the central region [Fig. 9(b)], the particles are generally larger and their size distributions do not change much with the barrel temperature. The longer cooling time has probably enhanced coalescence of the smaller particles and allowed contraction of the elongated PET domains back into spherical particles. It is noteworthy, in the sample extruded at 290°C, that the particle-size distributions near the skin and in the central region are very similar. This suggests that slow cooling of the extrudate is not favorable for fiber formation because it allows the elongated PET domains to shrink back into spherical particles.

Effect of die temperature

Three die temperatures, that is, 240, 260, and 290°C, were studied. The particle size near the skin [Fig. 10(a)] increases slightly with increasing die temperature. The increase in peak particle size, from 2 to 2.5 μm, between 260 and 290°C is smaller than is the effect of barrel temperature because of the short residence time of the melt in the die. The effect of die temperature on the particle-size distribution is not obvious in the central region of the extrudate [Fig. 10(b)]. Nevertheless, there is a slight drop in the peak intensity and an increase in the number of bigger particles for 290°C. This is probably a result of the slower solidification process, which enhances coalescence of smaller particles.

Effect of cooling medium

Four cooling media, namely, air, water (room temperature), ice water (0°C), and a mixture of liquid nitrogen and acetone (~−80°C), were used for this study. The melt was extruded directly into a beaker containing the liquid cooling media concerned; meanwhile, the extrudate was supported on a piece of wood after the die when using air as the cooling medium. No postextrusion drawing was applied on the extrudates; therefore, the flow was no longer elongational after the die. In fact, there was a slight radial flow due to die swell. Some coarse fibers were found near the skin, particularly in extrudates

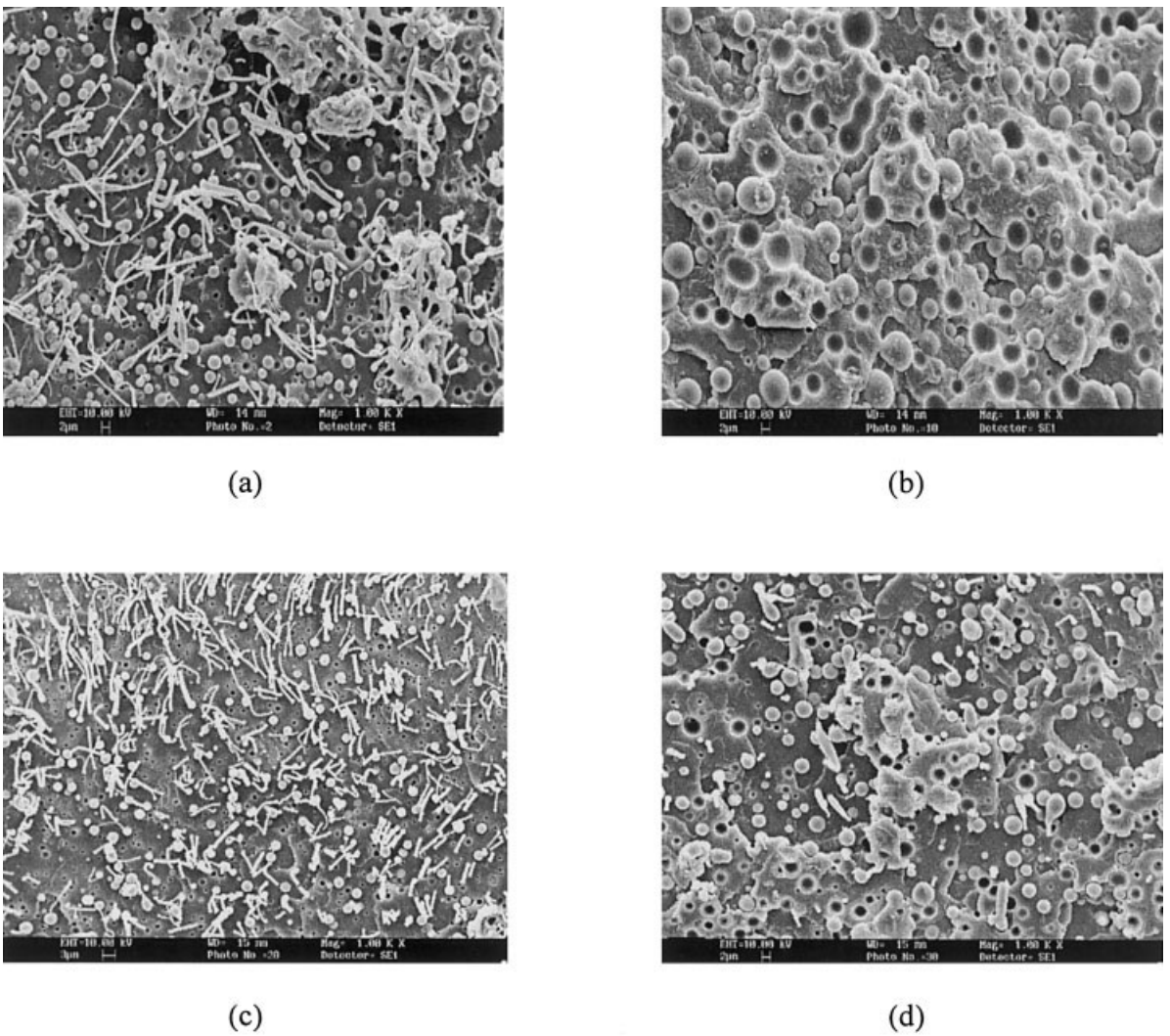

Figure 13 Cross-sectional morphology of PET/VM (20/80) extrudates prepared at different postextrusion drawing speeds: (a) 10 m/min, near skin; (b) 10 m/min, central region; (c) 25 m/min, near skin; (d) 25 m/min, central region.

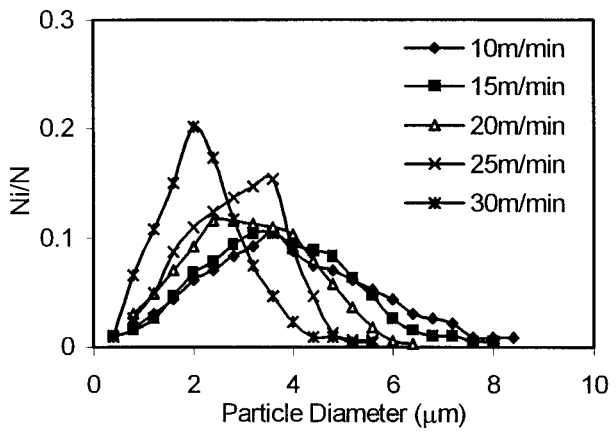

Figure 14 Effect of postextrusion drawing speed on PET particle-size distribution in central regions of PET/VM (20/80) extrudates.

cooled in the mixture of liquid nitrogen and acetone. Obviously, the fibers were formed inside the die, most probably due to the elongational flow generated at the convergent die entrance, and were preserved by the high cooling rate.

Basically, there are two mechanisms for fiber formation, that is, elongation and coalescence of the dispersed phase. Suppose that the dispersed PET domains are in the form of spherical particles at the die entrance where the cross section of the flow channel is wide and the speed of the flow is low. As the flow converges to the exit orifice, it is accelerated and a highly elongational flow is favorable for fiber formation.[24,25] An increase in the number of fibers always causes a corresponding decrease in the number of big particles, suggesting that elongation of big particles plays an important role in fiber formation. Although the phenomenon of coalescence of the dispersed PET phase has been observed after the die (Fig. 4), its frequency of occurrence is not very high. Neverthe-

TABLE I
Effects of Extrusion Conditions on Peak Particle Size of Dispersed PET Phase in PET/VM(20/80) Extrudates

Extrusion condition		Peak particle size (near skin) (μm)	Peak particle size (central region) (μm)
Barrel temperature	260°C	1.5	3.5
	270°C	2.5	3.5
	290°C	4.0	3.5
Die temperature	240°C	1.5	3.0
	260°C	2.0	3.0
	290°C	2.5	3.0
Cooling medium	Liquid N_2 + acetone	2.0	3.0
	Others	3.0	3.0
Screw speed	50 rpm	2.5	3.5
	100 rpm	1.5	2.0
	150 rpm	0.8	0.8
Postextrusion Drawing speed	15–20 m/min	2.5	3.5
	25–30 m/min	2.0	2.0

less, the possibility of vigorous coalescence along the upstream of the die cannot be ruled out.

Figure 11(a) shows the particle-size distribution near the skin. The liquid nitrogen and acetone mixture produces a narrower band of small PET particles, while the other three cooling media give a wider distribution with more large particles. The liquid nitrogen and acetone mixture was able to freeze the melt shortly after contact; therefore, the morphology is similar to that just after the die. The increase in particle size in the samples cooled in the other three media was probably a result of shrinkage of the elongated PET domains and coalescence of particles facilitated by the slower cooling rates. As expected, the particle-size distribution in the central regions of extrudates cooled in the different media does not vary significantly [Fig. 11(b)] because of slow cooling.

Effect of screw speed

The domain size of the dispersed PET phase decreases with an increasing screw speed and the PET particles near the skin are generally smaller than those in the central region (Fig. 12). The rotating screws input mixing energy into the melt, resulting in a decrease in the domain size of the dispersed phase along the barrel. The melt is then forced through the die. Some dispersed particles are deformed into fibrous domains or even broken into smaller particles as a result of capillary instability. If the size and shape of the minor phase during melt extrusion of incompatible polymer blends are the result of melt viscosity effects being balanced by interfacial tension, then the size of the minor phase will decrease continually to a final equilibrium size with an increasing input energy of mixing.[15,16] It was reported that the most significant particle-size deformation and disintegration processes took place within the first 2 min of mixing,[26] and after 2 min, very little reduction in the size of the minor phase was observed up to 20 min of mixing. Plochocki et al.[27] proposed that an abrasion mechanism was responsible for the early stage of the dispersion process and that the final domain size might be controlled by a dispersion–coalescence equilibrium.

Effect of postextrusion drawing

Hot stretching is very effective in transforming the dispersed minor phase into fibers.[25] Figure 13 shows the extrudates prepared at drawing speeds of 10 and 25 m/min, corresponding to draw ratios of 1.7 and 4.1, respectively. The higher drawing speed reduces the diameter of the PET fibers noticeably in the skin region; meanwhile, it does not change the size of the PET particles significantly. This is probably because the large PET particles in this region were deformed into fibers and only the smaller ones would survive the flow. In contrast, the PET particles in the central region of the extrudate prepared at 10 m/min are considerably bigger. Figure 14 shows the size distribution of the PET particles within the central regions of the extrudates prepared at different postextrusion drawing speeds. Furthermore, some coarse fibers are found in the central region of the extrudate prepared at 25 m/min [Fig. 13(d)]. This can be attributed to the fact that at a high drawing speed the flow remained highly elongational even after the die. It suppressed recovery of the elongated fibers formed in the die or

even increased the aspect ratio of those fibers. Also, reduction of the extrudate diameter, caused by the higher draw ratio, increased the cooling rate in the extrudate center, hence preventing the elongated PET domains from shrinking back to particles.

CONCLUSIONS

The typical morphology of the PET/VM(20/80) extrudate consists of three regions, that is, skin layer, intermediate region, and central region. The skin layer, about 10 μm thick, has a lower concentration of PET. The intermediate region, about 400 μm thick, has profuse PET fibers and some small PET particles. The central region, approximately 800 μm in diameter, contains mainly PET particles which are relatively larger. Elongation of particles appears to be a major mechanism of fiber formation because an increase in the number of fibers always results in a decrease of big particles. Although the phenomenon of coalescence was observed in the PET/VM (20/80) blend, it is difficult to assess its contribution to fiber formation. In comparison, coalescence is prevalent in the PET/KM (30/70) blend, forming PET platelets near the skin of the extrudate and irregular networks in the central region.

All the extrusion parameters show some effects on the peak particle size near the skin (Table I). In particular, screw speed is the most prevalent factor to change the particle size: The higher the screw speed, the smaller the particle size. A lower barrel temperature and a lower die temperature produce a smaller peak particle size and a large number of fibers. When different cooling media were used, only the mixture of liquid nitrogen and acetone gave a smaller peak particle size near the skin. The fast cooling rate had probably suppressed the shrinkage of elongated PET domains into big particles. Within the ranges of barrel temperatures, die temperatures, and cooling media used in this study, the size distribution of the PET particles did not change significantly in the central region. Meanwhile, a higher screw speed and postextrusion drawing speed reduced the peak particle size significantly. The former increases the mixing energy input and the latter keeps the flow in a highly elongational state after the die. Some fibers were found in the central regions of the extrudates prepared at a postextrusion drawing speed of 25 m/min or higher. In contrast, very few or no fibers were found in the central regions of the extrudates prepared under other extrusion conditions.

This project was supported by a CRCG grant from The University of Hong Kong.

References

1. Kiss, G. Polym Eng Sci 1987, 27, 410.
2. Blizard, K. G.; Baird, D. G. Polym Eng Sci 1987, 27, 653.
3. Weiss, R. A.; Huh, W.; Nicolais, L. Polym Eng Sci 1987, 27, 684.
4. Valenza, A.; La Mantia, F. P.; Paci, M.; Magagnini, P. L. Int Polym Process 1991, 6, 247.
5. Akhtar, S.; Isayev, A. I. Polym Eng Sci 1993, 33, 33.
6. Yang, Y.; Yin, J.; Li, B.; Zhuang, G.; Li, G. J Appl Polym Sci 1994, 52, 1365.
7. Petrovic, Z. S.; Farris R. J. Polym Adv Technol 1995, 6, 91.
8. Zaldua, A. M.; Eugenia Munoz, M.; Pena, J. J.; Santamaria, A. Macromol Rapid Commun 1995, 16, 417.
9. Champagne, M. F.; Dumoulin, M. M.; Utracki, L. A.; Szabo, J. P. ANTEC' 96, 1571.
10. Spreeuwers, H. R.; van der Pol, G. M. W. Plast Rubb Process Appl 1989, 11, 159.
11. Fakirov, S.; Evstatiev, M.; Schultz, J. M. Polymer 1993, 34, 4669.
12. Fakirov, S.; Evstatiev, M. Adv Mater 1994, 6, 395–398.
13. Evstatiev, M.; Nicolov, N.; Fakirov, S. Polymer 1996, 37, 4455.
14. Min, K.; White, J. L. Polym Eng Sci 1984, 24, 1327.
15. Wu, S. Polym Eng Sci 1987, 27, 335.
16. Taylor, G. I. Proc R Soc A 1934, 146, 501.
17. Lohfink, G. W.; Kamal, M. R. Polym Eng Sci 1993, 33, 1404.
18. Goldsmith, H. L.; Mason, S. G. In Rheology, Theory and Applications; Eirich, F. R., Ed.; Academic: New York, 1967; Vol. 4.
19. Gauthier, F.; Goldsmith, H. L.; Mason, S. G. Trans Soc Rheol 1971, 15, 297.
20. Bartram, E.; Goldsmith, H. L.; Mason, S. G. Rheol Acta 1975, 14, 776.
21. Tomotika, S. Proc R Soc 1935, 150, 322.
22. Chapleau, N.; Favis, B. D. J Mater Sci 1995, 30, 142.
23. Vainio, T. P.; Harlin, A.; Seppäläl, J. V. Polym Eng Sci 1995, 35, 225.
24. Grace, H. P. Chem Eng Commun 1982, 14, 225.
25. Gonzalez-Nunez, R..; Favis, B. D.; Carreau, P. J.; Lavallee, C. ANTEC '92, 1048.
26. Favis, B. D. J Appl Polym Sci 1990, 39, 285.
27. Plochocki, A. P.; Dagli, S. S.; Andrews, R. D. Polym Eng Sci 1990, 30, 741.